Article

Journal of
Nanoscience and Nanotechnology
Vol. 17, 2374–2381, 2017
www.aspbs.com/jnn

Preparation of Quantum Dots Hydrogel Nanocomposites with Improved Cytotoxicity

Abraham Gonzalez-Ruiz[1,2], Miguel A. Camacho-Lopez[1], and Miriam V. Flores-Merino[2,*]

[1] *Laboratorio de Fotomedicina, Biofotónica y Espectroscopía Laser de Pulsos Ultracortos. Facultad de Medicina, Universidad Autónoma del Estado de México (UAEM), Jesús Carranza y Paseo Tollocan s/n, Toluca, C.P. 50120, México*
[2] *Laboratorio de Biología Molecular y Celular. Centro de Investigación en Ciencias Médicas, UAEM, Jesus Carranza 200, Toluca, 50120, Mexico*

Nanocomposites are materials with unique properties and a wide range of applications. The combination of different nanostructures with traditional materials gives a variety of possibilities that should be analyzed. Especially, functional fluorescent semiconductor quantum dots (QDs) embedded in polymeric matrices have shown promising fluorescence and biocompatibility properties. These hybrid materials can be used in medical applications such as biodiagnostic and bioimaging. In this study, two hydrogels, one of polyethylene glycol diacrylate (PEGDA) and other of polyacrylamide (PAAm), were prepared with quantum dots of CdTe (4 nm of diameter) and characterized. The aim of this research was to analyze the optical properties of the nanocomposites and their cell viability. QDs nanocomposites were fabricated by a free radical polymerization process. The optical studies showed that the nanocomposites have well defined properties of fluorescence. To study the biocompatibility of the nanocomposites, metastatic B16f10 cell line were used and MTT assay was performed. The nanocomposites had a significant improved cell viability compared with QDs solutions.

Keywords: Polymer Network, Quantum Dots, Fluorescent, Nanocomposite, Hydrogel, Biocompatible.

1. INTRODUCTION

Semiconductor nanocrystals, usually known as QDs are attractive materials due to their unique physical and optical properties. Their characteristics depends on their size, and therefore in their quantum confinement effects.[1] Typically the QDs are a combination of II–VI, III–V and IV–VI group elements, for example tellurium selenide.[2,3] Some of their interesting properties include: fluorescence phenomena, adjustable wavelength spectrum, narrow and symmetrical emission (half width 15–40 nm), and a broad absorption spectrum that enables the simultaneous excitation of multiple fluorescent colors. Moreover, QDs are considerably brighter and resistant to photobleaching compared to fluorescent organic dyes widely used in biology applications.[4–7]

Recently, QDs are used in different fields of science such as biological labeling,[8] cancer detection[9] and bioimaging[10] among others. However, applications in the biomedical field have been hampered by their cytotoxicity implications. To reduce their inherent toxicity, QDs are typically conjugated with biological and low-cytotoxic ligands, including antibodies, peptides, sugars, polymers etc. As a result, the development of methods to obtain QDs-polymer hybrid materials with tunable optical properties is an active field of research.[11–13]

One of the materials used to coat QDs is a hydrogel matrix, which displays attractive properties such as: defined morphology, interconnected porosity, adjustable dimensions and the ability to imbibe large amount of solvent. Hydrogels are suitable for potential bio-applications due to its similarity with soft tissues and its good biocompatibility.[2,14] Their combination with QDs have found various applications such as: biosensing, bioimaging, tissue engineering, drug delivery, among others.[15,16]

The inclusion of QDs into a three-dimensional hydrogel matrix offers protection against different biological environments and provides unique photoelectronic properties.[14] There are a broad range of techniques that

*Author to whom correspondence should be addressed.

 1533-4880/2017/17/2374/008 doi:10.1166/jnn.2017.12709

have been employed to develop hydrogels with QDs embedded: ion exchange, grafting polymer to QDs, growth of QDs within polymer etc.[6] Also, polymers such as cellulose, poly(N-isopropylacrylamide), poly(ethylene glycol) diacrylate (PEGDA), poly(2-acrylamido-2-methyl-propane sulfonic acid) and others are used for surface passivation of QDs.[17–20]

In this work, highly fluorescent PEGDA and PAAm hydrogels with embedded QDs were prepared. The QDs of CdTe were encapsulated in the hydrogel matrices by an *in situ* polymerization process. Then, the swelling behavior and the optical properties (absorbance and fluorescence) were analyzed to determine their transparency and luminescent characteristics. Finally, the toxicity of the materials was studied by their exposition to the cancer cell line B16F10.

2. EXPERIMENTAL DETAILS

Materials. PEG (MW = 4000 g/mol, Polioles, México), 2,2'-Azobis(2-metilpropionamidina) dihydrochloride (AIBA; 98%; Sigma-Aldrich, USA), Acrylamide (99%; Polioles, Mexico), bisacrylamide (BIS; 99%; Sigma-Aldrich, USA), Ammonium Persulfate (APS; 99.8%; Sigma-Aldrich, USA) and Tetramethylenediamine (TEMED; 99%; Sigma-Aldrich, USA), quantum dots of CdTe functionalized with a carboxyl group (Sigma-Aldrich, USA), PTFE mold and multiband ultraviolet lamp 254/366 nm (Minerallight®, USA). All chemicals were used without prior purification.

2.1. Preparation of Hydrogels and QDs Nanocomposites

2.1.1. Poliethylenglycol Diacrylate (PEGDA) Hydrogels

Were produced by UV- photopolymerization. Linear polymer of PEGDA, previously synthesized, was homogenized in deionized water (0.1 g/ml) by magnetic stirring and sonicated for 5 minutes. Subsequently, AIBA photoinitiator (0.02 g/ml) was added into the solution. Finally, the synthesis was carried out by the exposition of the solution under ultraviolet light (366 nm) during 15 minutes.

2.1.2. PAAm (Polyacrylamide) Hydrogels

Were prepared by free radical polymerization of acrylamide (0.04 mg/ml), in the presence of bisacrylamide (1.5 μl/ml), APS (4 μg/ml) and TEMED (1 μl/ml).[21] The polymerization process took place during the first 30 minutes after the initiator was added.

2.2. QDs Nanocomposites

QDs in aqueous media (deionized water) were incorporated into the polymer network through direct *in situ* polymerization. Briefly, QDs solution (1.3 μM) was prepared before the polymerization process took place and stored in a tightly closed glass container, at a storage temperature of 2–8 °C, avoiding direct exposure to sunlight. PEGDA polymer (0.1 g/ml) and the initiator were added to the QDs solution and homogenized, then the mixture was exposed to UV-light in order to start the polymerization process. Similar procedure was performed for the PAAm nanocomposite. Nanocomposite hydrogels for cell culture experiments were synthetized under sterile conditions in a laminar flow cabinet class II.

2.3. Size and Morphological Characterization of QDs

The morphological study of the QDs was obtained by Transmission Electron Microscopy (TEM; Hitachi, USA) operating at 200 kV. Samples were prepared by placing a drop of the solution of nanoparticles (QDs) in a 300 mesh carbon coated copper grid. Size of quantum dots were confirmed by analysis of micrographs, additionally it was calculated from UV-vis data and using the following equation:

$$D = (9.8127 \times 10^{-7})\lambda^3 - (1.7147 \times 10^{-3})\lambda^2 + (1.0064)\lambda - (194.84)(\text{nm})^{22} \quad (1)$$

where D is the diameter of the particle and λ is the wavelength of maximum absorbance corresponding to the first exciton peak of the nanocrystal. The molar concentration of the nanocrystals in solution was determined by establishing the extinction coefficient and applying the Lambert-Beerś law. The methodology exposed by Yu and his coworkers was used.[22]

2.4. Chemical Characterization of Hydrogels by FTRI Spectroscopy

Dried samples of hydrogels were mixed with solid potassium bromide and obtained in a film form by mechanical means. Then, a spectrometer (Diamond GladiATR, Pike Technologies, USA) was used to record infrared (IR) spectra of the samples.

2.5. Physical Characterization of Hydrogels and QDs Nanocomposites

2.5.1. UV-VIS Spectroscopy

UV-VIS spectra of QDs solution, PEGDA hydrogels, PAAm hydrogels and QDs nanocomposites was obtained using a Perkin-Elmer Lambda 650 UV/VIS Spectrophotometer. The UV-VIS analysis of the materials was performed by acquiring their absorbance spectra in the wavelength of 200–800 nm.

2.5.2. Fluorescence Spectroscopy

The photoluminescence of the QDs solution and QDs nanocomposites was recorded on a Horiba Jobin Yvon FluoroMax-P spectrofluorometer with right-angle geometry. All samples were analyzed in a quartz cuvette (10 mm).

2.5.3. Swelling Behavior

A gravimetric method was employed for the swelling test. The equilibrium water content was measured in the hydrogels (PEGDA and PAAm) after immersing them in PBS (pH 7.4) at room temperature (25 ± 2 °C). Swelling kinetics (a temporal change in the water volume of the hydrogels) is expressed through the swelling ratio (Eq. (2)).

$$\text{swelling ratio} = \frac{M - M_d}{M_d} \tag{2}$$

Where M denotes the weight of the swollen sample, and M_d is the weight of the sample after polymerization was carried out.

2.5.4. Network Structure

Pore size and crosslinking density of the hydrogels (PEGDA, PAAm) was calculated based on the Flory-Rehner theory. For this purpose, samples were placed in a vacuum dryer until all the water contained in the material was absent. The density of the hydrogels was calculated using a buoyancy protocol.[23–25]

The hydrogel mesh size ξ was calculated using the following equation (Eq. (3)):

$$\xi = v_{2,s}\left[C_n\left(\frac{2\bar{M}_c}{\bar{M}_r}\right)\right]^{1/2} l \tag{3}$$

Where C_n is the Flory characteristic ratio, l is the carbon–carbon length and $\bar{M}_r$ is the molecular weight of the repeating unit of the polymeric chain.[26,27] The value of molecular weight between crosslinks, $\bar{M}_c$ was calculated from the swelling data (Eq. (4)) and the reported values from literature (Table I).

$$\frac{1}{\bar{M}_c} = \frac{2}{\bar{M}_n} - \frac{(v/v_1)[\ln(1+v_{2,s}) + v_{2,s} + \chi_1 v_{2,s}^2]}{v_{2,r}[((v_{2,s})/(v_{2,r}))^{1/3} - ((v_{2,s})/(v_{2,r}))]} \tag{4}$$

2.6. Cytotoxicity of Hydrogels and QDs Nanocomposites by MTT Assay

The highly metastatic subline cell B16F10 murine melanoma (European Collection of cell cultures, UK) was cultured in Dulbecco's Modified Eagle Medium (DMEM) supplemented with 10% fetal bovine serum, amphotericin (1 ug/ml) and sodium bicarbonate (3.7 g/L) under standard conditions.[28] The culture medium of the flasks was changed every 48 hours and cell viability was assessed through MTT assay. B16F10 cells were seeded at a density of 1×10^4 cells/200 μl and exposed to the samples for 24 h in standard conditions. Agar gel and cell culture plate were used as positive controls and cell culture plate without cells as negative control. The absorbance of untreated cells was considered as 100% cell viability.

3. RESULTS AND DISCUSSION

3.1. Preparation of Hydrogels and Chemical Characterization

During the formation of crosslinked PEGDA hydrogels, the photoinitiator (AIBA) was decomposed and free radicals were generated. The radicals attack the carbon–carbon double bond of acrylate end groups of PEGDA polymer, initiating the polymerization and subsequently creating PEGDA networks. The FT-IR spectra of PEGDA hydrogels showed that the carbon double bond at 1630 cm^{-1} almost disappeared (Fig. 1). This result indicated that some carbon double bonds still remain unrecated. The peaks at 1720 cm^{-1} and 1110 cm^{-1} were assigned to the C=O stretching vibration and the C–O asymmetric stretching vibration of group (–C–O–C–) respectively, the peak 2880 cm^{-1} is related to, C–H stretching vibration.

Polymerization of PAAm hydrogels was carried out by the same polymerization mechanism than PEGDA hydrogels. For this purpose APS was used as free radical generator and TEMED as a reaction accelerator. In the IR spectra the bands assigned to the N–H stretching vibration in –NH-group or –$CONH_2$ groups appeared at 3116–3340 and 1600 cm^{-1}. The C–H stretching band was characterized by the peak at 2931 cm^{-1} due to symmetric or asymmetric stretching vibration of the CH_2 groups. Bands at 1560 and 1406–1410 cm^{-1} were due to carboxylate group stretching of acrylate. At 1410–1450 cm^{-1}, a stretching of the C=O group from the acrylamide unit appears in the PAAm hydrogel spectra, the C–N stretching band was characterized by the peaks 1072–1311 cm^{-1} (Fig. 2).

3.2. Size and Morphological Characterization of QDs Solutions

The morphology of the QDs was investigated by TEM, the micrographs showed that nanoparticle have a size of 4 nm, and were monodispersed with spherical shape (Fig. 3). The size was also calculated from the absorption spectra of QDs. The nanocrystals exhibited a weak maximum

Table I. Parameters of PEGDA and PAAm hydrogels.

Sample	χ_1	$\bar{C}_n$	l	$\bar{M}_r$	$\bar{v}$	$\bar{v}_1$	$\bar{M}_n$
PEGDA Hydrogel	0.426	4	0.146 (nm)	44	0.84 (cm^3/g)	18.1 cm^3/mol in water	4000 (g/mol)
PAAm Hydrogel	0.48	8.8	15.4 Å	71.07	0.741 (cm^3/g)	18.1 cm^3/mol in water	36400 (g/mol)

Notes: χ_1—Polymer-solvent interaction parameter; $\bar{C}_n$—Flory characteristic ratio; l—Carbon–carbon bond length; $\bar{M}_r$—Molecular weight of repeat unit; $\bar{v}$—Specific volume of the polymer; $\bar{v}_1$—Molar volume of water; $\bar{M}_n$—Average molecular weight of the polymer before crosslinking.

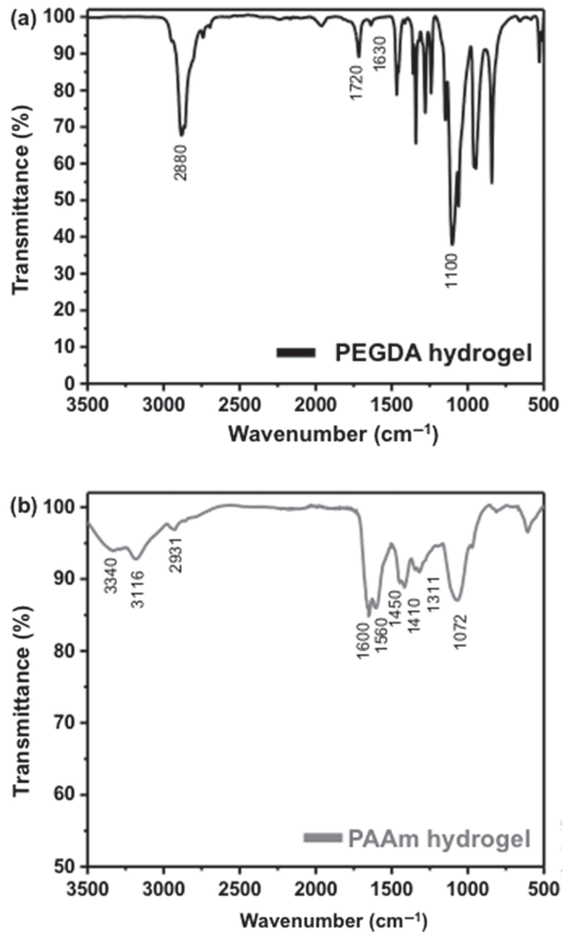

Figure 1. FT-IR spectra of (a) PEGDA hydrogel and (b) PAAm hydrogel.

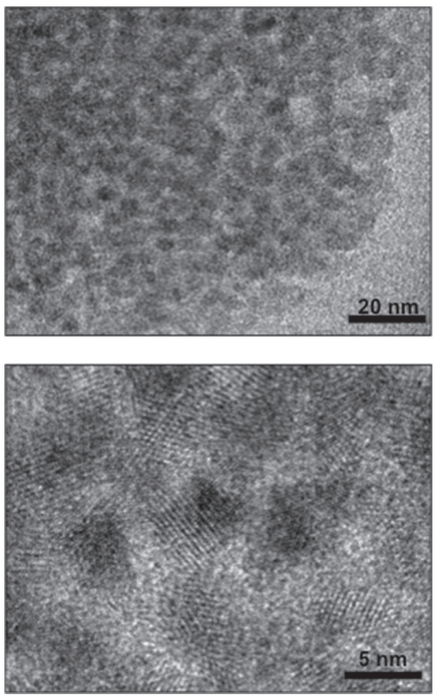

Figure 2. TEM micrographs of QDs solution (1.3 μM).

absorption for its first exciton transition because of the interactions between QDs and the functionalized carboxyl groups. This peak is observed around 540 nm and it was assigned to the 1s–1s electronic transitions (Fig. 4), from which the average particle size was calculated. The size of QDs was of 3.12 nm, similar to the value obtained by TEM.

3.3. Physical Characterization of Hydrogels and QDs Nanocomposites

Water soluble QDs were incorporated into PEGDA or PAAm hydrogels by carrying out *in situ* photopolymerization. A strong yellow color was formed throughout the hydrogels. The QDs embedded in hydrogels of PAAm and PEGDA have been scarcely studied, moreover the synthesis of PEGDA hydrogels using AIBA initiator has not been reported before for polymeric networks.

Optically PAAm and PEGDA hydrogels behave very similar. Both networks had a strong interaction in the same region of the UV spectrum (400 to 100 nm; Fig. 4) due to the water contained into their structure (water interacts strongly with UV radiation). It can be notice that the PAAm nanocomposite had a higher absorbance that PEGDA nanocomposite (Fig. 4). The absorbance of pure hydrogels was minimal (10%) in the regions of excitation (468 nm) and emission (770 nm) of QDs. As a result the optical interaction of PEGDA and PAAm hydrogels with QDs was not significant. Thus, these hydrogels are suitable for coating the QDs employed in this work.

3.4. Fluorescence Spectroscopy

The QDs exhibit its fluorescence maximum peak at a wavelength excitation of 468 nm (Fig. 5) and its maximum peak of emission at 777 nm (Fig. 6). The nanoparticles have a narrow and symmetric fluorescence spectra with FWHM (full width at half maximum) values in the range of 80–85 nm. This shows that CdTe are nearly monodispersed and homogenous (Fig. 6). In addition, the fluorescence spectra of the QDs nanocomposites had a bright red emission ($\lambda_{em} = 788$ nm) under blue light ($\lambda_{ext} = 468$ nm) excitation.

The PEGDA and PAAm nanocomposites show high fluorescence intensity, however lower than the QDs solution, most likely due to interactions between the QDs and the polymer matrix hydrogel. Clear fluorescence extinction intensity in the QDs nanocomposites (78% for PEGDA and 59% for PAAm nanocomposites, Fig. 6) is noticed. This could be explained by three main factors. First, immobilized QDs could migrate to the unbound water into the hydrogel structure. As a result, an energy transfer from the excited QDs to water molecules, that have

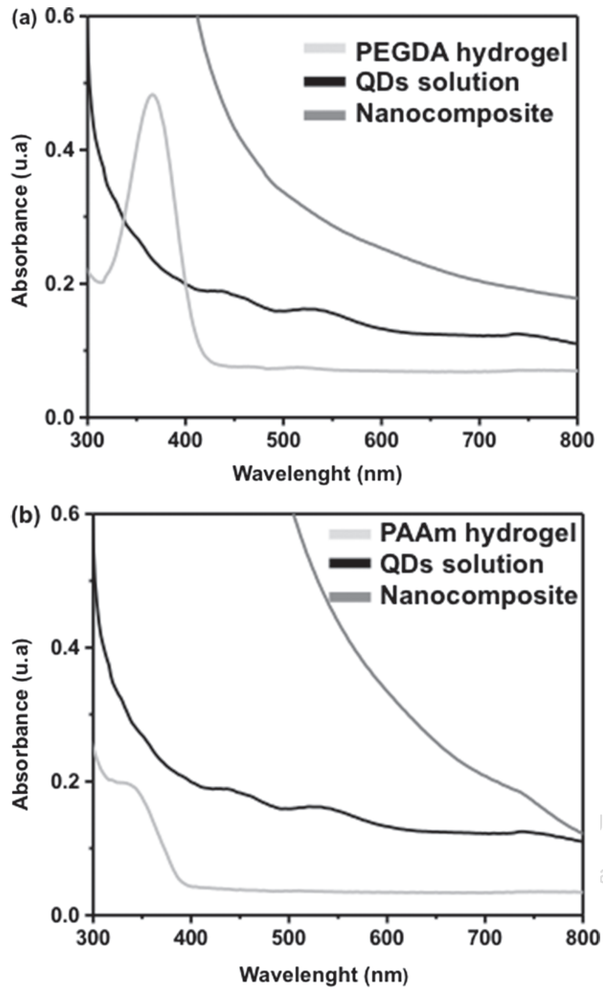

Figure 3. Optical analysis by UV-vis spectrophotometry. (a) Comparison among PEGDA hydrogels, PEGDA nanocomposite and QDs in solution (1.3 μM) and (b) comparison among PAAm hydrogel, PAAm nanocomposite hydrogel and QDs in solution (1.3 μM).

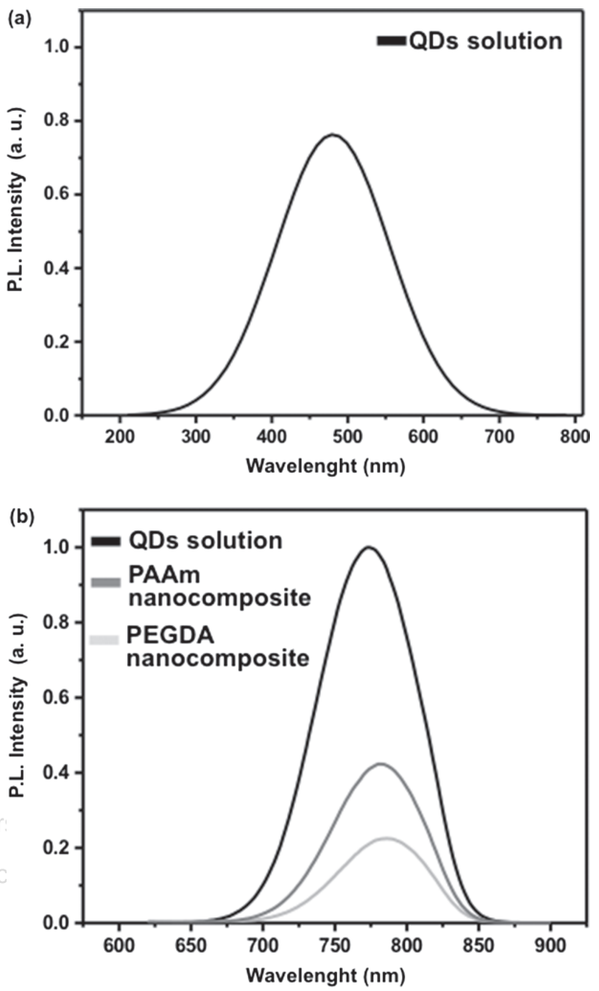

Figure 4. Fluorescence spectra: (a) excitation spectra of the QDs in solution (1.3 μM), allows us to determine the optimum wavelength of excitation in which QDs reach their fluorescence peak (468 nm) and (b) emission fluorescence spectra, comparison of PEGDA nanocomposite, PAAm nanocomposite and QDs solution (468 nm of excitation).

high dielectric constant, could take place. This generates a lower fluorescence response in the nanocomposites.

A second explanation is a slight increase in the energy bandgap of QDs due to the poor crystallinity of hydrogel materials that increases their number of localized states. As a result, the excited electrons in the valence band pass to the QDs conduction band with higher energy. Consequently, the fluorescence photons emitted by the nanocomposites have a different wavelength of emission to those emitted by the QDs solution.[29–31] To emphasize this phenomenon, a slight shift (10 nm) to the near infrared can be observed in the fluorescence spectrum emission of the QDs nanocomposites compared with the QDs solution (Fig. 6). Third, the phenomenon of fluorescence quenching of QDs nanocomposites, may be due to the high concentration of QDs embedded into the hydrogel. A high concentration of QDs can cause a self-extinction fluorescence phenomenon due to the transfer of energy between two particles of different size, for example: physical contact between two QDs.[14, 30, 32]

As have been noted, the PAAm nanocomposite has higher fluorescence intensity (increase of 43%, Figure 4(B)) than PEGDA nanocomposite. This can be explained because the PAAm hydrogel has a higher degree of crosslinking than the PEGDA hydrogel. Thus, the QDs were restricted into PAAm networks than into PEGDA hydrogels. Then, this could reduce the contribution of the effects of electron–hole recombination by non-radioactive pathways (heat) and decreases the effects of the energy transfer of excited QDs to water molecules.[14]

3.5. Swelling Behavior

To understand the structure of the materials and their interaction with the solvent, both hydrogels (PEGDA and PAAm) and nanocomposites were studied. The

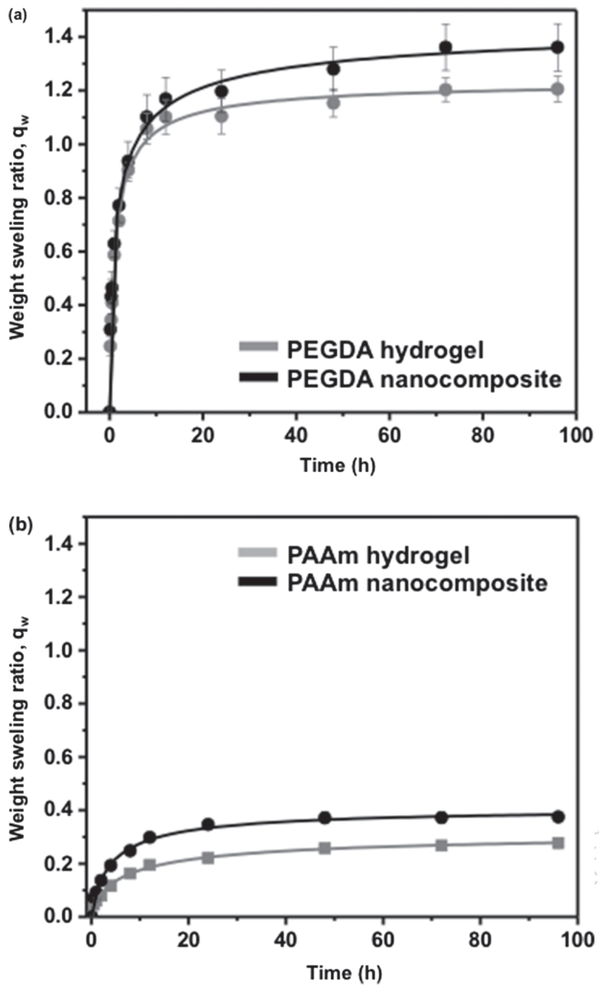

Figure 5. Weight swelling ratio of hydrogels and QDs nanocomposite hydrogels in PBS at 25 ± 2 °C. (a) PEGDA hydrogels and PEGDA nanocomposite hidrogel and (b) PAAm hydrogels and PAAm nanocomposite hydrogel ($n = 3$, sigmoidal fit, $r^2 = 0.99$).

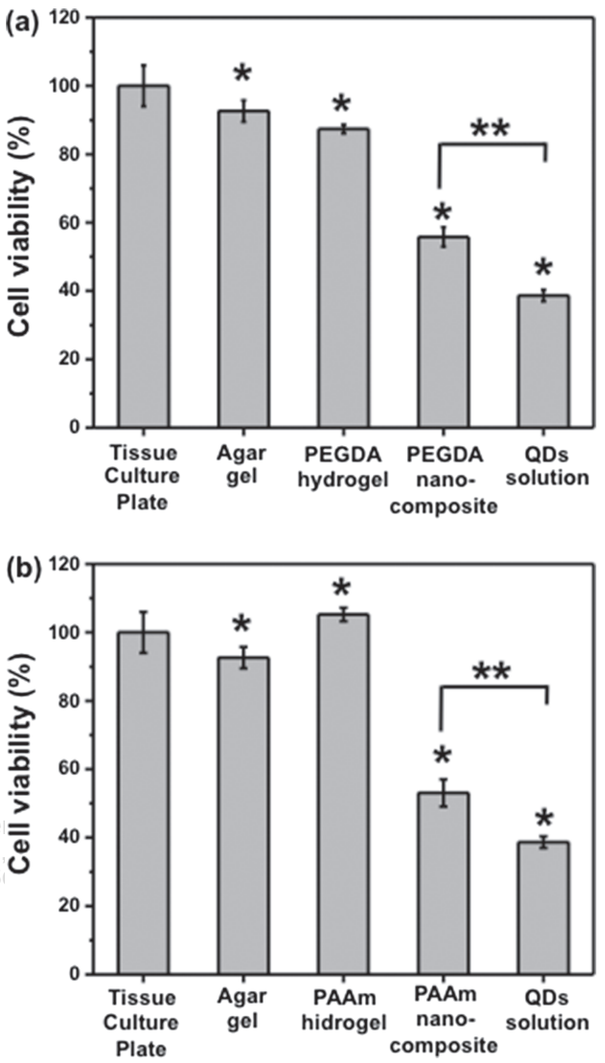

Figure 6. Cytotoxicity evaluation by MTT assay: (a) PEGDA hydrogel, QDs solution, PEGDA nanocomposite and (b) PAAm hydrogel and PAAm nanocomposite. Samples were exposed to the cell line B16F10 for 24 hours. The stars illustrate statistically significant differences compared to controls, i.e., cells not exposed to any material (tissue culture plate; t-test, $p < 0.05$) and hydrogel nanocomposites compared with QDs solution (t-student, $p < 0.05$).

nanocomposites showed higher swelling ratio compared to pure PEGDA and PAAm hydrogels. The PEGDA network with embedded QDs swelled approximately 0.133 more than the pure hydrogel. Similarly, the hydrogel of PAAm with encapsulated QDs swelled 0.357 more than pure hydrogel (Figs. 7–8). The results imply that QDs contribute to the higher swelling ratio of the hydrogels. This behavior can be attributed to the carboxyl groups in the surface of the QDs.

The hydrogels and nanocomposites of PAAm reach its swelling equilibrium at approximately 48 hours. The swelling ratio of PAAm hydrogels was 0.28 ± 0.02, meanwhile for the PAAm nanocomposite was 0.37 ± 0.018 (Fig. 7). PEGDA hydrogels and PEGDA nanocomposites reach equilibrium at approximately 72 hours with a maximum swelling ratio of 1.2 ± 0.04 and 1.36 ± 0.086, respectively (Fig. 8). PEGDA nanocomposite and hydrogels have a higher swelling ratio, almost six times more than the materials based on PAAm. Therefore, PEGDA materials have lower crosslinking density than PAAm hydrogels.

The average values of the mesh size of pure hydrogel (PEGDA, PAAm) were calculated from swelling data. PEGDA and PAAm mesh size were 4.59 ± 0.36 nm and $255 \pm 8\dot{A}$, respectively. The network mesh size of the hydrogels can affect the dispersion of the QDs inside the hydrogel matrix. Therefore, QDs with a diameter of roughly 4 nm are topologically restricted in PAAm hydrogel compared with PEGDA hydrogels, which have larger pores.

During the swelling test there was no signs of degradation and loss of weight in hydrogels and QDs

nanocomposites. Additionally, the solvent was analyzed over time by UV-visible spectrophotometry to monitor any release of QDs from the network. There was not any release of QDs optically detected (data not shown). These finding suggest that QDs nanoparticles keep retained in the hydrogel network, probably by secondary forces between polymer chains and QDs.

3.6. Cell Culture and MTT Assay

For future biological applications, especially clinical, materials must be non-toxic or exhibit low cytotoxicity. To evaluate the biocompatibility of the synthetized materials in this work, *in vitro* cytotoxicity MTT assay was conducted in B16F10 cells. The cytotoxicity of the QDs solutions, the hydrogels and nanocomposite hydrogels were compared. The B16F10 cell viability was significantly reduced ($38.68 \pm 1.69\%$, 24 h, $p < 0.05$) when exposed to a QDs solution (1.3 μM, 24 h) compared to those cells that were not exposed to any material ($100 \pm 6\%$, 24 h; Fig. 9). QDs toxicity can be attributed to surface corrosion when there is an interaction with cellular organisms. It has been described that QDs physicochemical properties in biological environments could be altered and chemically active toxic ions could be released, and cause irreversible cell damage.[33–35]

QDs toxicity was significantly inhibited ($p < 0.05$) when encapsulated in polymer matrices of PEGDA and PAAm. There were more viable cells in PEGDA nanocomposites, 17.5% more, than in solutions of QDs. Also, cell viability was increased by 15.2% in PAAm nanocomposites (Fig. 9). The inhibition of toxicity can be attributed to certain degree of neutralization of toxic ions (Cd^{+2}) by the polymeric network.[36] However, hydrogel nanocomposites still remain under the acceptance levels of cytotoxicity. It is noteworthy that studies of toxicity in QDs are hard to compare and generalize. There is a big controversy regarding the dependence of the QDs toxicity with the dose, duration, frequency of exposure and mechanisms of action.[34, 37, 38]

The excellent biocompatibility of PEGDA and PAAm hydrogels was expected.[39, 40] However, PEGDA networks have lower viability ($87.36 \pm 1.28\%$) than the PAAm hydrogels and controls. Possibly, some unreacted compounds in PEGDA hydrogels can elicit some toxicity in cells. The nanocomposites of PEGDA have a cell viability percentage of 55.8 ± 2.9, slightly higher but not significant, than the nanocomposite of PAAm $53.5 \pm 3.9\%$ (Fig. 9). Then, there is no difference between using the PAAm hydrogel or PEGDA hydrogel to reduce the overall QDs cytotoxicity. However, in the optical properties, the PAAm nanocomposite present higher fluorescence phenomena that PEGDA nanocomposite.

Despite the overall cell viability in the materials analyzed, it is also observed that the difference in viability between PEGDA networks and PEGDA nanocomposites (31.56%) is lower than between the PAAm hydrogels and PAAm nanocomposites (51.74%). These imply that PEGDA hydrogels could be more efficient to inhibit toxicity, even though they exhibit some cytotoxicity by their own.

4. CONCLUSIONS

QDs nanocomposites based on two different polymers were synthesized. The nanocomposites were stable with high water absorption, and exhibited good appearance, processability and handling. The hydrogel matrix structure of PEGDA and PAAm supplied cavities for the immobilization of the QD particles. Also, polymeric chains worked as a shell to maintain stability and protect their structure. It was demonstrated that nanocomposites have strong fluorescence emission under visible light in the dark and QDs toxicity was significantly inhibited by polymer matrix encapsulation. Cell viability was similar in PEGDA and PAAm nanocomposites, however QDs embedded in PAAm networks showed better optical properties.

Conflict of Interest

There are no conflicts of interest.

Autor Disclosure Statement

Authors have no competing interests to declare.

Acknowledgments: The authors gratefully acknowledge financial support from PRODEP (grant number: 103.51/13/6535) and UAEM (grant number: 3890/2015FS).

References and Notes

1. E. O. Chukwuocha, M. C. Onyeaju, and T. S. T. Harry, *WJCMP* 2, 2 (**2012**).
2. N. Sahiner, K. Sel, K. Meral, Y. Onganer, S. Butun, O. Ozay and C. Silan, *Colloids Surf A Physicochem Eng Asp.* 389 (**2011**).
3. D. R. Tilley, *Chem. N.Z.* 72, 4 (**2008**).
4. I. Costas-Mora, V. Romero, I. Lavilla, and C. Bendicho, *Trends Analyt Chem.* 57 (**2014**).
5. B. Kairdolf, A. M. Smith, H. T. Stokes, M. D. Wang, A. N. Young, and Y. S. Nie, *Annu. Rev. Anal. Chem.* 6 (**2013**).
6. N. Tomczak, D. Jańczewski, M. Han, and G. J. Vancso, *Prog Polym Sci.* 34, 5 (**2009**).
7. J. Rochira, M. Gudheti, T. Gould, R. Laughlin, J. Nadeau, and S. T. Hess, *J. Phys. Chem. C.* 111 (**2007**).
8. B. R. Liu, H. J. Chiang, Y. W. Huang, M. H. Chan, H. H. Chen, and H. J. Lee, *Pharmaceutical Nanotechnology* 1, 2 (**2013**).
9. P. Bae and B. Chung, *Nano Convergence* 1, 1 (**2014**).
10. P. Zrazhevskiy, M. Senawb, and X. Gao, *Chem. Soc. Rev.* 39, 11 (**2010**).
11. H. Zhang, R. Shi, A. Xie, J. Li, L. Chen, P. Chen, S. Li, F. Huang, and Y. Shen, *ACS Appl. Mater. Interfaces* 5, 23 (**2013**).
12. J. F. Luna-Martínez, D. B. Hernández-Uresti, M. E. Reyes-Melo, C. A. Guerrero-Salazar, V. A. González-González, and S. Sepúlveda-Guzmán, *Carbohydr. Polym.* 84, 1 (**2011**).
13. C. Chang, J. Peng, L. Zhang, and D. W. Panga, *Mater. Chem.* 19 (**2009**).

14. N. Patil, G. R. Saswati, U. Haldar, and P. De, *ACS Appl. Mater. Interfaces* 117, 50 **(2013)**.
15. M. Heine, A. Bartelt, O. T. Bruns, D. Bargheer, A. Giemsa, B. Freud, L. Scheja, C. Waurisch, A. Eychmüller, R. Reimer, H. Weller, P. Nielsen, and J. Heeren, *Beilstein J. Nanotechnol.* 5 **(2014)**.
16. M. Choi, J. W. Choi, S. Kim, S. Nizamoglu, S. K. Hahn, and S. H. Yun, *Nat. Photonics* 7 **(2013)**.
17. M. Muthiah, S. H. Park, M. Nurunnabi, J. Lee, Y. K. Lee, H. Park, B. Lee, J. J. Min, and I. K. Park, *Colloids Surf. B Biointerfaces* 116 **(2014)**.
18. J. Zhou and H. Li, *ACS Appl. Mater. Interfaces* 4, 2 **(2012)**.
19. Y. Liu, J. Yang, P. Zhang, C. Liu, W. Wanga, and W. Liu, *J. Mater. Chem.* 22, 2 **(2012)**.
20. Y. Gong, M. Gao, D. Wang, and H. Möhwald, *Chem. Mater.* 17, 10 **(2005)**.
21. J. Tse and A. Engler, *Wiley Interscience* **(2010)**.
22. W. W. Yu, L. Qu, W. Y. Guo, and X. Peng, *Chem. Mater.* 15, 14 **(2003)**.
23. D. Hariharan and N. A. Peppast, *Polymer* 37, 1 **(1996)**.
24. J. Wang and W. Wu, *Eur. Polym. J.* 41 **(2005)**.
25. F. Ganji, S. Vasheghani-Farahani, and E. Vasheghani-Farahani *Iranian Polymer Journal* 19, 5 **(2010)**.
26. A. Datta, Master Degree Thesis, Louisana, University of the State of Louisana **(2007)**.
27. T. Yang, PhD Thesis, Stockholm, Royal Institute of Technology in Stockholm **(2012)**.
28. I. Freshney, 6th edn., John Wiley and Sons Inc. Hoboken, England, NJ, USA **(2010)**.
29. M. Gou and M. Jiang, *Macromol. Rapid Commun* 31, 19 **(2010)**.
30. K. Kokado, A. Nagai, and Y. Chujo, *Macromolecules* 43, 15 **(2010)**.
31. J. Zhou and H. Li, *ACS Appl. Mater. Interfaces* 4, 2 **(2012)**.
32. R. Koole, P. Liljeroth, C. Donegá, D. Vanmaekelbergh, and A. Meijerink, *J. Am. Chem. Soc.* 128, 32 **(2006)**.
33. V. Breus, A. Pietuch, M. Tarantola, T. Basché, and A. Janshoff, *Beilstein J. Nanotechnoly* 6 **(2015)**.
34. A. Valizadeh, H. Mikaeili, M. Samiei, S. M. Farkhani, N. Zarghami, M. Kouhi, A. Akbarzadeh, and S. Davaran, *Nano Research Lett.* 7, 1 **(2012)**.
35. Y. Su, Y. He, H. Lu, L. Sai, Q. Li, W. Li, L. Wang, P. Shen, Q. Huang, and C. T. Fan, *J. Biomaterials* 30, 1 **(2009)**.
36. Y. Liu, J. Yang, P. Zhang, C. Liu, W. Wang, and W. Liu, *J. Matter. Chem.* 22 **(2012)**.
37. S. A. O. Gomes, C. S. Vieira, D. B. Almeida, J. R. Santos-Mallet, R. F. S. Menna-Barreto, C. L. Cesar, and D. Feder, *Sensors* 11, 12 **(2011)**.
38. J. P. Ryman-Rasmussen, J. E. Riviere, and N. A. Monteiro, *J. Invest Dermatology Adv.* 127, 1 **(2006)**.
39. A. J. Marzocca, A. L. Rodríguez, and M. A. Mancilla, *Polym Test.* 29, 1 **(2010)**.
40. N. A. Peppas, J. Z. Hilt, A. Khademhossini, and R. Langer, *Adv. Mater.* 18 **(2006)**.

Received: 8 May 2015. Accepted: 11 September 2015.